HHS Public Access

Author manuscript

Nat Neurosci. Author manuscript; available in PMC 2012 April 01.

Published in final edited form as:

Nat Neurosci. ; 14(10): 1285–1292. doi:10.1038/nn.2898.

Presynaptic Regulation of Quantal Size: K^+/H^+ Exchange Stimulates Glutamate Storage by Increasing Membrane Potential

Germaine Y. Goh[1], **Hai Huang**[3,*], **Julie Ullman**[1,2,*], **Lars Borre**[1], **Thomas S. Hnasko**[1], **Laurence O. Trussell**[3], and **Robert H. Edwards**[1]

[1]Departments of Physiology and Neurology Graduate Programs in Neuroscience, Cell Biology and Bioengineering University of California, San Francisco San Francisco, California 94158

[2]Graduate Program in Molecular and Cellular Biology University of California, Berkeley Berkeley, California 94720

[3]Oregon Hearing Research Center and Vollum Institute Oregon Health and Science University Portland, Oregon 97239

Abstract

The amount of neurotransmitter stored in a single synaptic vesicle can determine the size of the postsynaptic response, but the factors that regulate vesicle filling remain poorly understood. A proton electrochemical gradient ($\Delta\mu_{H+}$) generated by the vacuolar H^+-ATPase drives the accumulation of classical transmitters into synaptic vesicles. The chemical component of $\Delta\mu_{H+}$ (ΔpH) has received particular attention for its role in the vesicular transport of cationic transmitters as well as protein sorting and degradation. Thus, considerable work has addressed the factors that promote ΔpH. However, synaptic vesicle uptake of the principal excitatory transmitter glutamate depends on the electrical component of $\Delta\mu_{H+}$ ($\Delta\psi$). We now find that rat brain synaptic vesicles express monovalent cation/H^+ exchange activity that converts ΔpH into $\Delta\psi$, and this promotes synaptic vesicle filling with glutamate. Manipulating presynaptic K^+ at a glutamatergic synapse influences quantal size, demonstrating that synaptic vesicle K^+/H^+ exchange regulates glutamate release and synaptic transmission.

The response to release of neurotransmitter from a single synaptic vesicle (quantal size) can vary due to postsynaptic changes in receptors[1], but we know considerably less about the presynaptic regulation of quantal size through changes in vesicle filling with transmitter. Glutamate receptors are not saturated at the calyx of Held[2, 3] and synapses in the hippocampus and cerebellum[4, 5], indicating that changes in the amount of glutamate released per synaptic vesicle have the potential to influence miniature excitatory postsynaptic current

Address correspondence to Robert H. Edwards at Departments of Physiology and Neurology UCSF School of Medicine 600 16th St., Genentech Hall N272B San Francisco, CA 94158-2517 (415) 502-5687 telephone (415) 502-8644 fax robert.edwards@ucsf.edu.

*These authors contributed equally to the work presented.

Author Contributions Biochemical experiments were conducted by G.Y.G., J.U. and T.S.H. in the laboratory of R.H.E.; L.B. developed the measurement of ^{22}Na uptake. Electrophysiology experiments were performed by H.H. in the laboratory of L.O.T.

One-sentence summary: Synaptic Vesicle K^+/H^+ Exchange Increases Quantal Size

(mEPSC) amplitude. Indeed, synaptic vesicle enlargement due to alterations in endocytosis can increase quantal size[6, 7].

Previous work has suggested that changes in the expression of vesicular glutamate transporters (VGLUTs) may affect vesicle filling. Neural activity has been shown to regulate the expression of VGLUT mRNA[8], and decreased expression reduces quantal size in cultures from knock-out mice[9]. Heterozygous animals also show physiological and behavioral defects[10, 11]. However, we previously observed no difference in quantal size between VGLUT1 heterozygotes and wild type animals at hippocampal synapses[12]. Furthermore, a single VGLUT protein suffices to fill one synaptic vesicle in *Drosophila*[13], suggesting that VGLUT expression may influence the rate of vesicle filling rather than the gradient of transmitter achieved at equilibrium. However, changes in transport activity (rather than simply expression) have generally received little attention[14].

The transport of all classical transmitters into synaptic vesicles depends on a H^+ electrochemical gradient ($\Delta\mu_{H+}$) across the vesicle membrane. Generated by the vacuolar H^+-translocating ATPase (V-ATPase), $\Delta\mu_{H+}$ comprises both a chemical gradient (ΔpH) and membrane potential ($\Delta\psi$)[15]. The relative role of ΔpH and $\Delta\psi$ in turn varies with the stoichiometry of ionic coupling by different vesicular neurotransmitter transporters. Vesicular monoamine and acetylcholine transporters exchange two lumenal protons for one cationic transmitter, resulting in a greater dependence on ΔpH than $\Delta\psi$[16–18]. However, the V-ATPase initially produces $\Delta\psi$, which arrests its activity and prevents it from making ΔpH. The production of ΔpH thus requires the entry of an anion such as Cl^- to dissipate $\Delta\psi$, thereby activating the V-ATPase[19–22].

Although the stoichiometry of ionic coupling by the VGLUTs remains unknown, with the role of H^+ unclear, these carriers rely more on $\Delta\psi$ than ΔpH[20, 21]. As a result, glutamate entry acidifies synaptic vesicles[20, 23, 24], limiting the ability of the H^+ pump to create the $\Delta\psi$ required for VGLUT activity. Despite the importance of $\Delta\psi$ for vesicular glutamate transport, however, little is known about the mechanisms that promote its formation, or its role in the secretory pathway.

RESULTS

Synaptic vesicles express an electroneutral cation/H^+ exchange activity

A number of possible mechanisms might serve to dissipate the ΔpH accumulated during vesicular glutamate transport, and so increase the production of $\Delta\psi$ by the V-ATPase. First, a H^+ leak might simply allow the efflux of protons down their electrochemical gradient, but this would reduce $\Delta\psi$ as well as ΔpH[19]. Second, the efflux of anions from synaptic vesicles might itself create positive $\Delta\psi$, independent of the H^+ pump. This would require an outwardly directed anion gradient, and recent work using VGLUT1 reconstituted into artificial membranes has shown that chloride efflux can promote vesicular glutamate transport[25], although its physiological significance remains unknown. Alternatively, the influx of cytoplasmic cation might increase $\Delta\psi$ either by permeation through a channel, or through stoichiometrically coupled H^+ exchange[20]. Coupled cation/H^+ exchange has the advantage that it uses ΔpH to drive cation uptake, and if electroneutral, does not dissipate

$\Delta\psi$, allowing the V-ATPase to increase $\Delta\psi$ at the expense of the ΔpH that accumulates during vesicular glutamate transport.

A cation/H^+ exchange mechanism predicts that a cation gradient will drive the formation of ΔpH in the absence of the V-ATPase. To test this hypothesis, we pre-loaded synaptic vesicles (LP2; see Methods) with high Na^+ at pH 7.4, inhibited the H^+ pump with bafilomycin A1 and diluted the vesicles (LP2/Na) into buffer (pH 7.4) without Na^+ (Fig. 1). Using the quenching of acridine orange fluorescence within acidic compartments, Figure 1a shows that the outwardly directed Na^+ gradient suffices to acidify synaptic vesicles in the absence of V-ATPase activity, whereas dilution into buffer with Na^+ eliminates this effect, demonstrating its dependence on a Na^+ gradient.

Although consistent with coupled cation/H^+ exchange, cation-driven acidificaton might simply reflect the development of negative $\Delta\psi$ due to the efflux of Na^+, followed by H^+ influx driven by membrane potential. If driven by $\Delta\psi$, H^+ flux should increase in the presence of H^+ ionophore carbonyl cyanide chlorophenylhydrazone (CCCP). Normalized to paired controls, however, the rate of acidification in CCCP is 0.931 ± 0.069 ($p = 0.42$ by two-tailed, paired t-test, n=3) (Fig. 1b). CCCP thus has no effect on the rate of acidification, effectively excluding a role for $\Delta\psi$ in the H^+ entry driven by cation efflux. Na^+ efflux and H^+ influx thus do not appear to occur through distinct mechanisms, but rather through stoichiometrically coupled and presumably electroneutral exchange.

After the formation of stable ΔpH, addition of external Na^+ alkalinizes the vesicles, demonstrating flux reversal. We took advantage of this phenomenon to compare monovalent cations. At all concentrations tested (5, 20 and 150 mM), Na^+ and Li^+ demonstrate greater alkalinization than K^+ (Fig. 1d and data not shown). Characterization of the initial rate yields a K_m of 4.10 ± 2.35 mM for Na^+ and 140 ± 118 mM for K^+ (Hill coefficient = 1.04 ± 0.10 and 1.18 ± 0.30, respectively). Differences in recognition of the two cations presumably account for the inability of K^+ to reverse completely the ΔpH created by an outwardly directed Na^+ gradient, but the Vmax for both cations is remarkably similar (1.96 ± 0.64 afu/s for Na^+ versus 2.16 ± 1.10 afu/s for K^+) (Fig. 1e,f).

To test further the possibility that cation flux through a channel drives H^+ translocation, we determined whether synaptic vesicles express an endogenous cation conductance. We created an artificial ΔpH by loading the vesicles with ammonium tartrate (100 mM), inhibiting the V-ATPase with bafilomycin and diluting the membranes into buffer lacking NH_4^+--the efflux of NH_3 due to dilution rapidly produces ΔpH (Fig. 2a,b). The H^+ ionophore CCCP does not dissipate the ΔpH formed by dilution, presumably because the initial efflux of H^+ rapidly creates lumen-negative $\Delta\psi$ that opposes further efflux (Fig. 2a,c). Further, the inability of CCCP to dissipate ΔpH even after dilution into 150 mM K gluconate (Fig. 2b,c) indicates that synaptic vesicles lack an endogenous K^+ channel which can shunt the developing $\Delta\psi$. As controls, the addition of K^+ ionophore valinomycin to dilution buffer containing 150 mM K^+ immediately triggers H^+ efflux which increases in the presence of CCCP, and valinomycin does not have this effect in buffer lacking K^+ (Fig. 2a,b). The inability of K^+ to dissipate ΔpH in the absence of valinomycin excludes a role for endogenous channels in the observed cation-driven H^+ flux by synaptic vesicles.

Cation/H^+ exchange increases synaptic vesicle membrane potential

To assess a role for cation/H^+ exchange in the presence of the H^+ pump and specifically on the glutamatergic population of synaptic vesicles, we used ATP and glutamate to acidify synaptic vesicles. In the presence of 1 mM MgATP and 2 mM chloride (to activate allosterically the VGLUTs), 10 mM glutamate produces substantial acidification (Fig. 3a). The acidification is specific for glutamatergic vesicles because under the same conditions, the closely related aspartate (which is not recognized by VGLUTs) causes no acidification[24]. The subsequent addition of 50 mM Na^+ or K^+ then produces a steady alkalinization, whereas $NMDG^+$ as control has no effect (Fig. 3a). Similar to results obtained in the absence of V-ATPase activity, both cations thus alkalinize and Na^+ has a greater effect than K^+ at low concentrations (Fig. 3a). Acidification by the ATPase increases the concentration of both cations required for alkalinization, but the results show that cation/H^+ exchange can reduce the ΔpH of glutamatergic synaptic vesicles despite the presence of an active H^+ pump.

By selectively dissipating ΔpH, cation/H^+ exchange should increase Δψ generated by the V-ATPase. To measure Δψ, we used the potential-sensitive, ratiometric fluorescent dye oxonol VI, focusing on K^+ due to its physiological relevance as the most abundant cytoplasmic cation. Activation of the V-ATPase with ATP increases the fluorescence ratio of oxonol VI, indicating formation of a positive membrane potential, and the addition of K^+ (50 mM) causes a further increase of ~40% (Fig. 3b). To determine whether Δψ increases due to dissipation of ΔpH and secondary activation of the V-ATPase, we used ammonia, which acts as a weak, permeant base to dissipate ΔpH. Indeed, ammonium also increases the fluorescence ratio of oxonol VI, indicating an increase in Δψ (Fig. 3b). Further, the presence of ammonia reduces the effect of K^+ and vice versa, indicating that they act through a common mechanism. K^+/H^+ exchange across synaptic vesicle membranes thus dissipates ΔpH to increase Δψ.

Monovalent cations increase glutamate uptake into synaptic vesicles

The ability of cation/H^+ exchange to increase Δψ suggests that cations should stimulate glutamate transport into synaptic vesicles. We thus compared the effects of K gluconate and choline gluconate on ^{3}H-glutamate uptake by synaptic vesicles, using either 2 mM KCl or choline Cl to provide allosteric activation of the VGLUTs. The use of K^+ rather than Na^+ minimized the activity of any contaminating plasma membrane excitatory amino acid transporters, which rely on Na^+ co-transport. As shown in Figure 4a, external K^+ stimulates glutamate uptake into synaptic vesicles by ~50%, and the uptake as well as the stimulation by K^+ are blocked by Evans Blue, an inhibitor of the VGLUTs[26]. We also observed no specific uptake of ^{3}H-aspartate, which is recognized by the plasma membrane glutamate transporters but not by the VGLUTs, confirming the specificity of the assay for vesicular glutamate transport. To determine whether the loading of synaptic vesicles with membrane-impermeant choline gluconate has unanticipated consequences, we also examined glutamate uptake after pre-loading with Na gluconate or the more physiological NaCl, and observed little effect on glutamate uptake, although internal NaCl slightly reduces the stimulatory effect of external K^+ (Fig. S1). We thus used vesicles pre-loaded with choline gluconate for all subsequent experiments.

To characterize the effect of K^+ on glutamate uptake, we examined the time course and find that the stimulation by K^+ increases over time, with less effect at 1–2 minutes than at later times, when it approaches 100% after background subtraction (Fig. 4b). Consistent with a primary effect on thermodynamic equilibrium, kinetic analysis demonstrates only a small effect of K^+ on the K_m and no effect on V_{max} (Fig. 4c). The analysis of dose-response also shows a linear relationship up to 150 mM K^+ (Fig. 4d). To assess the effects of Na^+ and Li^+ in this assay, we inhibited any contaminating Na^+-dependent plasma membrane glutamate transporters with DL-*threo*-β-benzyloxyaspartic acid (TBOA) (Fig. S2). Consistent with the acridine orange experiments, we find that Na^+ and Li^+ also stimulate vesicular glutamate uptake (Fig. 4e), and the similar effect of all three cations in this assay presumably reflects the use of higher, saturating concentrations (150 mM) at a later time point than in the real-time fluorescence measurements of ΔpH (50 mM), where Na^+ and Li^+ have a bigger effect than K^+.

The stimulation of glutamate uptake into synaptic vesicles by monovalent cations could result from an allosteric effect on VGLUT activity, or an increase in the driving force for transport. Direct allosteric regulation should influence the kinetics of transport or exhibit saturation, but K^+ does not have much effect on the observed kinetics (Fig. 4c), and the dose-response to K^+ shows no evidence of saturation (Fig. 4d). To determine whether K^+ stimulates glutamate uptake by influencing $\Delta\mu_{H+}$, we again used ammonia to convert ΔpH to Δψ. By itself, 20 mM NH_4^+ stimulates glutamate uptake, consistent with the primary dependence of the VGLUTs on Δψ rather than ΔpH (Fig. 5a). The extent of stimulation resembles that produced by 150 mM K^+. We then tested whether K^+ can stimulate glutamate transport in the presence of ammonia and found that although not eliminated, the stimulation by K^+ is substantially reduced by ammonia (Fig. 5a). Conversely, the stimulation by ammonia is reduced by K^+, corroborating the studies with oxonol VI which suggest that potassium and ammonia act through a common mechanism. Since ammonia dissipates ΔpH, the results suggest that ΔpH is required for the full stimulation by K^+, and that H^+ efflux drives K^+ entry through K^+/H^+ exchange. The residual stimulation of glutamate uptake by K^+ in the presence of NH_4^+ (Fig. 5a) can be attributed to the same exchange mechanism driven solely by a K^+ gradient rather than by both ΔpH and a K^+ gradient.

To determine whether a cation channel even has the potential to influence vesicular glutamate transport, we measured glutamate uptake in the presence of the K^+ ionophore valinomycin and 15 mM K^+, a concentration of K^+ that alone has little effect (Fig. 4d). Valinomycin has no effect on vesicular glutamate transport under these conditions (Fig. 5b) as well as at physiological concentrations of K^+ (data not shown), indicating that even if a cation channel were present, it would not promote vesicle filling with glutamate. In contrast, the K^+/H^+-exchanging ionophore nigericin markedly increases glutamate uptake even in 15 mM K^+ (Fig. 5b), confirming that K^+/H^+ exchange potently stimulates vesicular glutamate transport.

Presynaptic K^+ increases quantal size at the calyx of Held

If cations increase glutamate uptake by synaptic vesicles, presynaptic K^+ should influence quantal size. We thus performed paired recordings at the calyx of Held, a giant

glutamatergic terminal in the brainstem auditory pathway where it is possible to dialyze cytosolic contents by whole-cell patch clamp, and simultaneously measure the postsynaptic response. Since glutamate receptors at this synapse are not saturated by a single quantum of transmitter[2, 3], it should be possible to detect changes in mEPSC amplitude due to changes in vesicle filling.

Immediately after break-in to whole-cell mode, we observed no difference in mean mEPSC amplitude with the presynaptic pipette containing either high K^+ or $NMDG^+$ solution ($p=0.76$). Moreover, with high K^+ solution, the mEPSC remains stable over 25–30 minutes of recording (Fig. 6a,d,g; $p>0.05$, $n=4$). With dialysis of the terminal in $NMDG^+$ rather than K^+, however, mEPSC amplitude gradually declines by over 30% (Fig. 6b,e,g; $p<0.001$, $n=5$). Normalized to the values observed immediately after break-in, mEPSC size is clearly lower in $NMDG^+$ than K^+ ($p<0.05$), and the cumulative frequency distribution shifts to the left with dialysis in $NMDG^+$ but not K^+ (Fig. 6d,e). The difference in mEPSC amplitude is remarkably consistent with the stimulation of vesicular glutamate transport by cations observed *in vitro* using either choline or $NMDG^+$ as control (Figs. 4a and S3). As also predicted from the dissipation of ΔpH by cations in the presence of an active H^+ pump (Fig. 3a) and from the direct measurement of glutamate uptake (Fig. S3), the presence of 10 mM Na^+ in NMDG does not reproduce the effect of 130 mM K^+ (Fig. 6), further supporting the importance of K^+ under physiological conditions.

EIPA inhibits synaptic vesicle cation/H^+ exchange

Stoichiometric cation/H^+ exchange predicts that, just as a cation gradient can drive H^+ flux, a H^+ gradient should also drive the accumulation of cations. We thus measured the uptake of $^{22}Na^+$ by synaptic vesicles acidified with glutamate to isolate the glutamatergic population. We observe more $^{22}Na^+$ uptake in the presence of glutamate than in aspartate as control (Fig. 7a), suggesting that vesicle acidification mediated by the VGLUTs drives $^{22}Na^+$ influx. Indeed, the VGLUT inhibitor Evans Blue blocks the stimulation by glutamate (Fig. 7b). Although the effect of glutamate appears modest, the ionophore monensin, which directly exchanges H^+ for Na^+, only increases uptake by ~70%, indicating that the endogenous activity is substantial. The VATPase inhibitor bafilomycin also blocks glutamate-stimulated $_{22}Na^+$ uptake (Fig. 7b), confirming that the uptake depends on $\Delta\mu_{H+}$ generated by the V-ATPase, and arguing against the role for a channel since cation uptake by a channel should increase (rather than decrease) in the absence of a positive $\Delta\psi$ produced by the V-ATPase. Further, the dissipation of ΔpH by ammonia, which should have little effect on a cation channel, blocks the stimulation of $^{22}Na^+$ uptake by glutamate (Fig. 7b), consistent with its dependence on ΔpH.

To characterize the proteins responsible for synaptic vesicle cation/H^+ exchange, we took advantage of the available pharmacology. In particular, we compared the effects of glutamate and aspartate on $^{22}Na^+$ uptake in the presence of different inhibitors. The K^+ channel inhibitor tetraethylammonium (TEA) and Na^+ channel inhibitor tetrodotoxin (TTX), as well as TRP channel inhibitors ruthenium red (RuR) and 2-aminoethoxydiphenyl borate (2-APB) all have no effect on glutamate-induced $^{22}Na^+$ uptake (Fig. 7c), consistent with the evidence against a cation channel.

Coupled cation/H^+ exchange suggests the involvement of Na^+/H^+ exchangers (NHEs). The NHEs include both plasma membrane isoforms involved in the regulation of cell pH and osmolyte concentration, and intracellular isoforms that recognize K^+ as well as Na^+ but remain poorly understood in terms of their physiological role[27, 28]. In general, the NHEs show sensitivity to inhibition by the amiloride analogue 5-(N-ethyl-N-isopropyl)amiloride (EIPA)[28]. However, most studies of NHE pharmacology have examined the uptake of trace $^{22}Na^+$, requiring only low micromolar or submicromolar concentrations of compounds such as EIPA that act as competitive inhibitors. Physiological levels of Na^+ or K^+ would require much higher concentrations of EIPA, at which nonspecific effects may arise. We thus used $^{22}Na^+$ to assess the EIPA sensitivity of cation uptake by synaptic vesicles. EIPA inhibits glutamate-activated $^{22}Na^+$ uptake in the very low micromolar range, with no effect of much higher concentrations on $^{22}Na^+$ uptake in the presence of aspartate (Fig. 7d), indicating that the EIPA-inhibitable uptake resides specifically on glutamatergic vesicles. EIPA also inhibits $^{22}Na^+$ uptake more potently than amiloride (Fig. 7e), a feature characteristic of the NHEs[28]. In addition, we tested the effect of EIPA on cation stimulation of vesicular glutamate uptake. Using higher concentrations of EIPA (50 μM) to compete with the higher concentrations of cation used (150 mM), we found that EIPA also inhibits the stimulation of glutamate uptake by Na^+ and K^+ (Fig. 7f). Further, EIPA inhibits the cation/H^+ exchange activity responsible for the Na^+ gradient-driven flux of H^+ observed in the acridine orange assay (Fig. 1c). NHEs thus appear to mediate the stimulation of vesicular glutamate transport by cation/H^+ exchange.

To assess the dependence of quantal size on NHE activity, we used the calyx of Held. Since the presynaptic solution contained 130 mM K^+ rather than the trace amounts of ^{22}Na used for measurements of flux, we added 50–100 μM EIPA to the presynaptic pipette. In contrast to the same solution without EIPA, dialysis with a high K^+ solution containing EIPA gradually reduces mEPSC amplitude (Fig. 6c,f,g; $p<0.01$, $n=4$), very similar to the low K^+ solution. EIPA thus inhibits the effect of K^+ on quantal size, supporting the involvement of an intracellular NHE.

DISCUSSION

The results presented here describe a novel, presynaptic mechanism for the regulation of quantal size (Supp. Fig. S4). During vesicular glutamate transport, ΔpH accumulates, opposing the activity of the H^+ pump and hence limiting the storage of glutamate. Cation/H^+ exchange dissipates ΔpH but, due to its electroneutrality, spares Δψ. As a result, continuing activity of the V-ATPase increases selectively Δψ, effectively converting ΔpH into Δψ. Since vesicular glutamate transport depends primarily on Δψ, electroneutral cation/H^+ exchange increases vesicle filling with glutamate.

Several observations show that synaptic vesicles express an electroneutral cation/H^+ exchange activity. First, the efflux of preloaded cation down a concentration gradient drives H^+ entry, suggesting that cation flux is directly coupled to H^+ exchange. Alternatively, this might reflect the production of negative Δψ by cation efflux, followed by the Δψ-driven H^+ influx, but the H^+ ionophore CCCP affects neither the rate nor the extent of acidification, effectively excluding a Δψ-driven process. A high conductance H^+ channel might occlude

the effect of CCCP, and synaptic vesicles can exhibit a H^+ leak. However, CCCP greatly increases H^+ efflux in the presence of an electrical shunt (Fig. 2), indicating that the endogenous H^+ conductance cannot occlude the effect of the ionophore. CCCP should thus have stimulated H^+ entry if it depended on $\Delta\psi$, and the lack of effect supports direct, electroneutral cation/H^+ coupling.

Second, we do not detect a cation conductance on synaptic vesicles. CCCP does not dissipate ΔpH produced by the efflux of NH_3 because the development of negative $\Delta\psi$ opposes net H^+ efflux. This is true even in the presence of external K^+, indicating that cation entry through endogenous channels cannot shunt the developing $\Delta\psi$. Only the addition of K^+ ionophore valinomycin in the presence of external K^+ allows significant H^+ efflux, demonstrating that we would have detected an endogenous cation channel if one were present. Although we cannot exclude the presence of a cation channel on synaptic vesicles, the results suggest that any conductance must be small.

Third, inhibition of the V-ATPase with bafilomycin reduces $^{22}Na^+$ uptake. Since VATPase activity makes $\Delta\psi$ more positive, cation uptake through a channel should increase if the V-ATPase is inhibited. The reduction in $^{22}Na^+$ uptake by bafilomycin thus indicates that $\Delta\psi$ does not drive flux. Rather, the decrease in $^{22}Na^+$ uptake produced by ammonia supports a selective role for ΔpH, consistent with cation/H^+ exchange and the resulting dissipation of ΔpH activates the V-ATPase, shifting the expression of $\Delta\mu_{H+}$ from ΔpH to $\Delta\psi$. Indeed, oxonol VI fluorescence documents the effect of K^+ on $\Delta\psi$ and the occlusion of this effect by ammonia suggests that K^+, like NH^+_4, increases $\Delta\psi$ by decreasing ΔpH. Taken together, the results indicate that in the presence of an active V-ATPase, a stoichiometrically coupled, electroneutral cation/H^+ exchange mechanism increases $\Delta\psi$. By acidifying synaptic vesicles with glutamate, we also find that cation/H^+ exchange occurs on the glutamatergic population.

Cation/H^+ exchange provides a mechanism to convert the ΔpH produced by glutamate accumulation back into $\Delta\psi$ that drives vesicular glutamate transport. Indeed, we find that K^+ increases the uptake of glutamate into synaptic vesicles in a manner consistent with thermodynamic effects on the driving force. The time course shows greater stimulation by K^+ at later time points, and K^+ has no effect on V_{max}, although it does reduce K_m slightly. Although a kinetic parameter, the K_m of vesicular glutamate transport has previously been shown to correlate with $\Delta\psi$[29]. The effect of K^+ on K_m may thus reflect a change in $\Delta\psi$.

To determine whether the stimulation of VGLUT activity by K^+ involves the observed increase in $\Delta\psi$, we again used ammonia. Like K^+, ammonia stimulates glutamate uptake, and the two effects partially occlude each other, suggesting that dissipation of ΔpH accounts for the stimulation by K^+, consistent with cation/H^+ exchange. Alternatively, K^+ influx through a channel could increase $\Delta\psi$ and reduce ΔpH by inhibiting the H^+ pump. Indeed, recent work has suggested that the cation channel TRPM7 found on cholinergic synaptic vesicles has a role in the regulation of acetylcholine release, but this was attributed to protein-protein interactions and changes in release rather than vesicle filling[30]. We would not have detected the effect of a cation channel expressed on a small subset of synaptic vesicles, but find no evidence for a cation channel functional on the majority of synaptic

vesicles. Further, valinomycin does not enable K^+ to stimulate vesicular glutamate transport, indicating that a channel would not increase vesicle filling even if one were present. In contrast, nigericin strongly augments glutamate uptake, demonstrating the potency of electroneutral K^+/H^+ exchange.

The manipulation of presynaptic cytosol at the calyx of Held further supports a physiological role for vesicle K^+ flux in glutamate release. Dialysis of the presynaptic terminal with a solution containing $NMDG^+$ rather than K^+ reduces quantal size, and the magnitude of the effect resembles that observed biochemically. Although the parallel effects *in vitro* and *in vivo* might not seem surprising, manipulation of presynaptic Cl^- at the calyx of Held does not affect quantal size[31] despite considerable previous work *in vitro* demonstrating a role for Cl^- in the allosteric regulation of VGLUTs[23, 29]. Allosteric regulation by Cl^- presumably affects kinetics rather than thermodynamics, and equilibrium may thus have a more important role in the determination of quantal size. Cation/H^+ exchange thus appears to have a greater impact on glutamatergic neurotransmission than the extensively documented effects of Cl^-.

The results implicate an intracellular NHE in transmitter release. NHEs catalyze the electroneutral exchange of cation for H^+ (1:1), and plasma membrane isoforms (NHE1–5), which recognize Na^+ but not K^+, have important roles in the regulation of cytoplasmic pH[28]. In contrast, the intracellular isoforms NHE6–9 recognize K^+ as well as Na^+[32–34], and remain poorly understood. The intracellular yeast homologue Nhx1 contributes to Na^+ resistance and membrane trafficking[35, 36]. In mammalian vestibular hair cells, which are surrounded by endolymph containing high concentrations of K^+, a fraction of NHE6 and 9 on the plasma membrane regulates cell pH[32]. However, we still understand little about the physiological role of NHEs on intracellular membranes.

The apparent electroneutrality of synaptic vesicle cation/H^+ exchange and its recognition of K^+ as well as Na^+ implicate the activity of an intracellular NHE. The sensitivity of $^{22}Na^+$ uptake by synaptic vesicles to low micromolar concentrations of EIPA but not a series of known channel blockers support the role of an intracellular NHE[28]. Further, EIPA blocks the ability of high presynaptic K^+ to maintain mEPSC amplitude at the calyx of Held. Together with the characterization of synaptic vesicle cation/H^+ exchange activity, the pharmacology thus implicates an intracellular NHE in the determination of quantal size. Interestingly, the endosomal isoforms NHE6 and 9 have recently been implicated in brain development and human disease. Mutations in *nhe6* cause an X-linked recessive form of mental retardation with seizures[37], and polymorphisms in *mhe9* have been associated with autism[38]. Genetic association studies have also implicated NHE9 in attention-deficit/hyperactivity disorder[39]. The role of NHE activity in filling synaptic vesicles with glutamate now raises the possibility that these mutations may interfere with behavior by disrupting neurotransmitter release. Although not originally identified in a proteomic analysis of synaptic vesicles[40], NHE6 has indeed been recently reported in synaptic vesicles storing both GABA and glutamate[41]. Further, recent work in *C. elegans* has demonstrated the role for an NHE homologue in chemical signaling from intestinal epithelial cells to muscle[42]. In this case, protons are the signal, and their release does not require vesicle fusion, but cation/H^+ exchange by synaptic vesicles may have evolved from this mechanism.

The results indicate a mechanism to control the expression of $\Delta\mu_{H+}$ as either ΔpH or Δψ, suggesting a novel intracellular role for NHEs. Although differences in the subcellular location of ClC isoforms might contribute to the variation in pH of different membranes, lysosomal transporter ClC-7 and a bacterial homologue both exhibit a stoichiometry of 2 Cl^- : 1 H^+[43, 44], and intracellular isoforms ClC-4 and −5 show similar H^+ coupling[45, 46]. Differences in coupling stoichiometry by the intracellular ClCs thus seem unlikely to account for the observed variation in organelle pH. However, the combination of a ClC (or Cl^- channel) with opposing NHE activity that converts ΔpH back into Δψ, could provide an explanation for the wide range of ΔpH: dominance of NHE over ClC activity may confer the relatively small ΔpH of early endosomes, and dominance of ClC over NHE the larger ΔpH of late endosomes and lysosomes. Consistent with this hypothesis, none of the intracellular NHEs have yet been localized to lysosomes—NHE6 and 9 reside earlier in the endocytic pathway, and NHE7 and 8 in the Golgi complex[33, 34]. The regulation of NHE and ClC trafficking may thus contribute to the observed variation in ΔpH across membranes of the secretory pathway.

In addition, intracellular NHE activity has the potential to augment Δψ to a greater extent than predicted by the activity of the H^+-ATPase alone. Electroneutral K^+/H^+ exchange predicts $log_{10}\left(\left[H^+\right]_i/\left[H^+\right]_o\right)=log_{10}\left(\left[K^+\right]_i/\left[K^+\right]_o\right)$ at equilibrium, and assuming the H^+ pump can create $\Delta\mu_{H+}=\left(log_{10}\left[H^+\right]_i/\left[H^+\right]_o\right)+\Delta\psi/\left(2.3RT/F\right)^{-3}$ where R is the gas constant, T the absolute temperature, and F Faraday's constant,

$$3-log_{10}\left(\left[H^+\right]_i/\left[H^+\right]_o\right)=\Delta\psi/\left(2.3RT/F\right)$$

or

$$3-log_{10}\left(\left[K^+\right]_o/\left[K^+\right]_i\right)=\Delta\psi/\left(2.3RT/F\right).$$

A 10-fold inwardly directed gradient of K^+ would thus increase the maximum Δψ possible by ~60 mV. Rather than simply modulating the expression of $\Delta\mu_{H+}$ as either ΔpH or Δψ, intracellular NHE activity together with an inwardly directed K^+ gradient can therefore augment the membrane potential produced by the vacuolar H^+ pump.

The focus of most previous work on ΔpH rather than Δψ reflects the established role of ΔpH in processes such as ligand-receptor dissociation and lysosomal degradation. However, the importance of Δψ for vesicular glutamate transport and the identification of cation/H^+ exchange as a mechanism to promote Δψ suggest that changes in Δψ may not simply reflect the unintended consequence of regulating ψpH. Rather, Δψ across membranes of the secretory pathway may serve as the primary driving force for additional processes which as yet remain poorly understood.

METHODS

Materials

Bafilomycin A1 was obtained from EMD Biosciences, Oxonol VI from Invitrogen, and other chemicals from Sigma. ^{22}NaCl and [^{3}H]L-glutamate were obtained from Perkin-Elmer, and HT-200 Tuffryn filters and Supor 200 filters from Pall. Choline gluconate was made by titration of choline bicarbonate with gluconic acid to pH 7.4, choline glutamate and choline aspartate by titration of choline base with glutamic or aspartic acid, respectively.

Synaptic vesicle preparation

Synaptic vesicles were isolated by differential centrifugation from rat brain synaptosomes lysed in hypotonic buffer, as previously described[47]. Briefly, the brains of 16 four week old Sprague-Dawley rats were homogenized in 320 mM sucrose, 4 mM HEPES-Tris, pH 7.4, 1 mM $MgCl_2$, 1 mM EGTA (homogenization buffer) containing 1 μg/ml pepstatin A and 200 μM PMSF using nine strokes of a Kontes #22 glass-Teflon homogenizer at 900 rpm. After sedimentation at 1,000 g_{max} for 10 min, the supernatant (S1) was collected, recentrifuged at 12,000 g_{max} for 15 min, and the resulting supernatant (S2) as well as the dark brown middle part of the pellet discarded. The remaining pellet (P2) was washed by resuspension in 6 ml homogenization buffer per brain, sedimenting at 13,000 g_{max} for 15 min and again discarding the supernatant (S2') and dark brown part of the pellet. The pellet (P2') was then resuspended in 0.6 ml homogenization buffer per brain, and 9 volumes of ice-cold water added along with 1 M HEPES-Tris, pH 7.4 to a final concentration of 8 mM. After incubation on ice for 30 min, the suspension was homogenized using 5 strokes at 3,000 rpm, and centrifuged at 33,000 g_{max} for 20 min. The supernatant (lysate supernatant, or LS1) was immediately collected and centrifuged at 260,000 g_{max} for 2 h. The resultant pellet (lysate pellet, or LP2) was resuspended in 400–500 μl 150 mM choline gluconate containing 10 mM HEPES-Tris, pH 7.4 (or other buffers as specified in Figs. 1, 2 and S1) by pipetting through progressively narrower micropipette tips, and finally by 3 passes through a 25 gauge needle. LP2 was frozen in liquid N_2 for storage at −80°, and thawed on ice before use. Protein concentration was determined by Bradford assay using bovine serum albumin as standard. To assess loading with K^+ by freeze-thaw, we used titration with external K^+ in the presence of nigericin to determine the external concentration that eliminates net H^+ flux as measured by acridine orange fluorescence (see below). By this method, freeze-thaw in 150 mM K gluconate results in only 25–50 mM lumenal K^+ (data not shown), and we presume that other cations behave similarly. These experiments were approved by the UCSF Institutional Animal Care and Use Committee.

ΔpH and Δψ measurements

ΔpH and Δψ were measured by acridine orange and oxonol VI fluorescence, respectively. 100–200 μg LP2 was added to 1.5 ml 150 mM choline or NMDG gluconate (unless otherwise indicated), 10 mM HEPES-Tris, pH 7.4 and either 5 μM acridine orange or 100 nM oxonol VI, and the reaction stirred at 30°C. A decrease in the fluorescence of acridine orange reflects generation of an inside-acidic ΔpH; an increase in the fluorescence ratio of oxonol VI reflects generation of an inside-positive Δψ. In the experiments using LP2 loaded with high Na^+ (which did not involve MgATP), 4 mM $MgSO_4$ and 0.5 μM bafilomycin A1

were included in the external solution. Acridine orange fluorescence was excited at 492 nm and emission detected at 530 nm; oxonol VI was excited at 560 nm and emission detected at 640 and 615 nm using a Hitachi F-4500 fluorescence spectrophotometer.

Glutamate transport assay

Unless indicated otherwise, the standard assay buffer for glutamate uptake contained (in mM): 148 choline, NMDG, Na or K gluconate, 2 choline or KCl, 4 MgATP, 10 HEPES-Tris, pH 7.4, 1 choline glutamate (unless otherwise indicated), and 40 μCi/ml [^{3}H]L-glutamate. When specified, Na gluconate and Li gluconate were used at 150 mM and $(NH_4)_2$ tartrate at 10 mM. Transport was initiated by the addition of 100 μg LP2 protein to 200 μl reaction buffer (pre-warmed to 30°C), the reaction incubated at 30°C for 10 min (unless otherwise indicated) and stopped by rapid filtration and washing four times with 2 ml each cold 150 mM HEPES-Tris, pH 7.4. Radioactivity was detected by liquid scintillation, and background transport measured in the presence of 100 μM Evans Blue subtracted from the data unless otherwise specified. Within each experiment, each condition was assayed in triplicate, and at least three independent experiments were performed using at least two different synaptic vesicle preparations.

$^{22}Na^+$ transport assay

The standard assay buffer for $^{22}Na^+$ transport contained (in mM): 148 choline gluconate, 2 choline chloride, 10 choline glutamate, 4 MgATP, 10 HEPES-Tris, pH 7.4, 0.1 ouabain, 0.1 bumetanide and 175 nM ^{22}NaCl (5 μCi/ml). Transport was initiated by adding 100 μg LP2 to 200 μl reaction buffer (pre-warmed to 30°C). The mixture was incubated at 30°C for 10 min (unless otherwise indicated) and the reaction stopped by rapid filtration followed by four washes each with 1.5 ml cold 150 mM HEPES-Tris, pH 7.4. Radioactivity was detected by liquid scintillation, and non-specific background at 0 min subtracted from all the data presented. At least three independent experiments were performed, each in triplicate.

mEPSC recordings

The handling and care of animals for these experiments was in accordance with procedures approved by Oregon Health Sciences University. *Slice preparation*: 180–200 μm-thick coronal slices containing the medial nucleus of the trapezoid body (MNTB) were prepared from P9–P12 Wistar rats as previously described[48, 49]. Slices were cut in cold artificial cerebrospinal fluid (ACSF) (composition, in mM: 230 sucrose, 25 glucose, 2.5 KCl, 3 $MgCl_2$, 0.1 $CaCl_2$, 1.25 NaH_2PO_4, 25 $NaHCO_3$, 0.4 ascorbic acid, 3 *myo*-inositol, and 2 Na-pyruvate, pH 7.4 bubbled with 5% CO_2/95% O_2), incubated for 30–60 minutes at 35°C and thereafter at room temperature.

Recordings—Slices were transferred to a recording chamber and perfused with recording ACSF containing (in mM) NaCl 125, KCl 2.5, $CaCl_2$ 2, $MgCl_2$ 1, NaH_2PO_4 1.25, ascorbic acid 0.4, myo-inositol 3, Na pyruvate 2, $NaHCO_3$ 25, glucose 25, and bubbled with 5% CO_2/95% O_2. To record mEPSCs, the ACSF contained 0.5 μM strychnine and 10 μM SR95531, 50 μM D-AP5 and 0.5 μM TTX. Slices were viewed using Dodt contrast optics and a 40× water immersion lens, and recordings made using an Axon Multiclamp 700B amplifier (Molecular Devices). The postsynaptic recording pipette solution contained (in

mM) Cs-CH_3SO_3 110, CsCl 5, $MgCl_2$ 1, MgATP 4, TrisGTP 0.4, Tris-phosphocreatine 14, EGTA 5, HEPES 10, adjusted to pH 7.30 with CsOH (290 mOsm). The K^+-based solution in the presynaptic electrodes contained (in mM) K-CH_3SO_3 110, KCl 20, MgATP 4, Tris-GTP 0.3, Na_2-phosphocreatine 5, $Tris_2$-phosphocreatine 9, EGTA 0.2, HEPES 10, glutamate 1, adjusted to pH 7.30 with KOH. The low Na^+, K^+ based presynaptic solution contained (in mM) K-CH_3SO_3 110, KCl 20, MgATP 4, Na_3-GTP 0.3, $Tris_2$-phosphocreatine 14, EGTA 0.2, HEPES 10, glutamate 1, adjusted to pH 7.30 with KOH. The K^+-free presynaptic solution contained (in mM) NMDG-CH_3SO_3 110, NMDG-Cl 20, MgATP 4, Tris-GTP 0.3, Na_2-phosphocreatine 5, $Tris_2$-phosphocreatine 9, EGTA 0.2, HEPES 10, glutamate 1, adjusted to pH 7.30 with NMDG. In some experiments, 20 μM Alexa-594 was also added to the presynaptic solution. Calyces were clamped at −80 mV (for K-based solution, corrected for junction potential of 10 mV) or −75 mV (for NMDG-based solution, corrected for a 5 mV junction potential). Postsynaptic cells were clamped at − 82 mV (including junction potential of 12 mV). Two tests were used to confirm recording from a calyx: first, the fluorescent dye fill of the calyx was visualized at the end of each recording; second, a depolarizing voltage was injected into the calyx and increased mEPSC frequency or a large postsynaptic response was measured. Signals were filtered at 10 kHz and sampled at 20 kHz. During recordings with NMDG or EIPA, the mEPSC frequency dropped to a variable extent. For example, in the 10 mM Na^+ condition, these changes were, for K^+, 7.7 ± 3.2 Hz (range 2.4 – 16.9) at 0–2' and 6.8 ± 0.5 Hz (range 5.7 – 7.8) at 25–30' (p=0.76, paired t-test); for $NMDG^+$, 8.2 ± 2.4 Hz (range 1.1 – 15.9) at 0–2' and 2.7 ± 1.6 Hz (range 0.4 – 8.8) at 25–30' (p=0.015, paired t-test); and for EIPA, 13.2 ± 2.9 Hz (range 5.1 – 18.6) at 0–2' and 2.6 ± 0.8 Hz (range 0.7 – 4.8) at 25–30' (p=0.017, paired t-test). These changes might reflect at least in part detection problems as mEPSC amplitude dropped, but this possibility was not explored further here. *Data Analysis*: mEPSCs were detected using a sliding template algorithm[49], with a rise time of 0.2 ms and decay of 0.5 ms, threshold of 4× noise SD, using Axograph X. Data were analyzed using Clampfit 9.2 (Molecular Devices) and Igor 6.0 (Wavemetrics), and expressed as mean ± SEM.

Statistical analysis

All mean data were obtained from at least three measurements using at least two different synaptic vesicle preparations. Error bars represent s.e.m. Statistical significance was assessed by two-tailed paired t-tests, unless otherwise indicated in the figure legends. Significance levels used are *p < 0.05, **p < 0.01, ***p < 0.0001. “NS” denotes differences that are statistically not significant (p > 0.05).

Supplementary Material

Refer to Web version on PubMed Central for supplementary material.

Acknowledgements

We thank J. Orlowski, S. Schuldiner and members of the Edwards lab for many thoughtful discussions, S. Manandhar and F. Farrimond for technical assistance and R.P. Seal for critical reading of the manuscript. This work was supported by fellowships from A*STAR (to G.Y.G.) and the American Heart Association (to L.B.), and by grants from NIDCD and NINDS (to L.O.T.) and from NIMH and NIDA (to R.H.E.).

REFERENCES

1. Bredt DS, Nicoll RA. AMPA receptor trafficking at excitatory synapses. Neuron. 2003; 40:361–379. [PubMed: 14556714]
2. Ishikawa T, Sahara Y, Takahashi T. A single packet of transmitter does not saturate postsynaptic glutamate receptors. Neuron. 2002; 34:613–621. [PubMed: 12062044]
3. Wu XS, et al. The origin of quantal size variation: vesicular glutamate concentration plays a significant role. J. Neurosci. 2007; 27:3046–3056. [PubMed: 17360928]
4. Conti R, Lisman J. The high variance of AMPA receptor- and NMDA receptor-mediated responses at single hippocampal synapses: evidence for multiquantal release. Proc. Natl. Acad. Sci. U S A. 2003; 100:4885–4890. [PubMed: 12682300]
5. Sargent PB, Saviane C, Nielsen TA, DiGregorio DA, Silver RA. Rapid vesicular release, quantal variability, and spillover contribute to the precision and reliability of transmission at a glomerular synapse. J. Neurosci. 2005; 25:8173–8187. [PubMed: 16148225]
6. Karunanithi S, Marin L, Wong K, Atwood HL. Quantal size and variation determined by vesicle size in normal and mutant Drosophila glutamatergic synapses. J. Neurosci. 2002; 22:10267–10276. [PubMed: 12451127]
7. Steinert JR, et al. Experience-dependent formation and recruitment of large vesicles from reserve pool. Neuron. 2006; 50:723–733. [PubMed: 16731511]
8. De Gois S, et al. Homeostatic scaling of vesicular glutamate and GABA transporter expression in rat neocortical circuits. J. Neurosci. 2005; 25:7121–7133. [PubMed: 16079394]
9. Wojcik SM, et al. An essential role for vesicular glutamate transporter 1 (VGLUT1) in postnatal development and control of quantal size. Proc. Natl. Acad. Sci. U S A. 2004; 101:7158–7163. [PubMed: 15103023]
10. Moechars D, et al. Vesicular glutamate transporter VGLUT2 expression levels control quantal size and neuropathic pain. J. Neurosci. 2006; 26:12055–12066. [PubMed: 17108179]
11. Seal RP, et al. Sensorineural deafness and seizures in mice lacking vesicular glutamate transporter 3. Neuron. 2008; 57:263–275. [PubMed: 18215623]
12. Fremeau RT Jr. et al. Vesicular glutamate transporters 1 and 2 target to functionally distinct synaptic release sites. Science. 2004; 304:1815–1819. [PubMed: 15118123]
13. Daniels RW, et al. A single vesicular glutamate transporter is sufficient to fill a synaptic vesicle. Neuron. 2006; 49:11–16. [PubMed: 16387635]
14. Brunk I, et al. The first luminal domain of vesicular monoamine transporters mediates G-protein-dependent regulation of transmitter uptake. J. Biol. Chem. 2006; 281:33373–33385. [PubMed: 16926160]
15. Saroussi S, Nelson N. Vacuolar H(+)-ATPase-an enzyme for all seasons. Pflugers Arch. 2009; 457:581–587. [PubMed: 18320212]
16. Johnson RG, Carty SE, Scarpa A. Proton: substrate stoichiometries during active transport of biogenic amines in chromaffin ghosts. J. Biol. Chem. 1981; 256:5773–5780. [PubMed: 7240171]
17. Knoth J, Zallakian M, Njus D. Stoichiometry of H+-linked dopamine transport in chromaffin granule ghosts. Biochemistry. 1981; 20:6625–6629. [PubMed: 6458332]
18. Parsons SM. Transport mechanisms in acetylcholine and monoamine storage. Faseb Journal. 2000; 14:2423–2434. [PubMed: 11099460]
19. Johnson RG, Pfister D, Carty SE, Scarpa A. Biological amine transport in chromaffin ghosts. Coupling to the transmembrane proton and potential gradients. J. Biol. Chem. 1979; 254:10963–10972. [PubMed: 40978]
20. Maycox PR, Deckwerth T, Hell JW, Jahn R. Glutamate uptake by brain synaptic vesicles. Energy dependence of transport and functional reconstitution in proteoliposomes. J. Biol. Chem. 1988; 263:15423–15428. [PubMed: 2902091]
21. Tabb JS, Kish PE, Van Dyke R, Ueda T. Glutamate transport into synaptic vesicles. J. Biol. Chem. 1992; 267:15412–15418. [PubMed: 1353494]

22. Van Dyke RW. Proton pump-generated electrochemical gradients in rat liver multivesicular bodies. Quantitation and effects of chloride. J. Biol. Chem. 1988; 263:2603–2611. [PubMed: 2963813]
23. Hartinger J, Jahn R. An anion binding site that regulates the glutamate transporter of synaptic vesicles. J. Biol. Chem. 1993; 268:23122–23127. [PubMed: 8226829]
24. Hnasko TS, et al. Vesicular glutamate transport promotes dopamine storage and glutamate corelease in vivo. Neuron. 2010; 65:643–656. [PubMed: 20223200]
25. Schenck S, Wojcik SM, Brose N, Takamori S. A chloride conductance in VGLUT1 underlies maximal glutamate loading into synaptic vesicles. Nat. Neurosci. 2009; 12:156–162. [PubMed: 19169251]
26. Chaudhry FA, Boulland JL, Jenstad M, Bredahl MK, Edwards RH. Pharmacology of neurotransmitter transport into secretory vesicles. Handb. Exp. Pharmacol. 2008:77–106. [PubMed: 18064412]
27. Brett CL, Donowitz M, Rao R. Evolutionary origins of eukaryotic sodium/proton exchangers. Am. J. Physiol. Cell Physiol. 2005; 288:C223–239. [PubMed: 15643048]
28. Orlowski J, Grinstein S. Diversity of the mammalian sodium/proton exchanger SLC9 gene family. Pflugers Arch. 2004; 447:549–565. [PubMed: 12845533]
29. Wolosker H, de Souza DO, de Meis L. Regulation of glutamate transport into synaptic vesicles by chloride and proton gradient. J. Biol. Chem. 1996; 271:11726–11731. [PubMed: 8662610]
30. Krapivinsky G, Mochida S, Krapivinsky L, Cibulsky SM, Clapham DE. The TRPM7 ion channel functions in cholinergic synaptic vesicles and affects transmitter release. Neuron. 2006; 52:485–496. [PubMed: 17088214]
31. Price GD, Trussell LO. Estimate of the chloride concentration in a central glutamatergic terminal: a gramicidin perforated-patch study on the calyx of Held. J. Neurosci. 2006; 26:11432–11436. [PubMed: 17079672]
32. Hill JK, et al. Vestibular hair bundles control pH with (Na+, K+)/H+ exchangers NHE6 and NHE9. J. Neurosci. 2006; 26:9944–9955. [PubMed: 17005858]
33. Nakamura N, Tanaka S, Teko Y, Mitsui K, Kanazawa H. Four Na+/H+ exchanger isoforms are distributed to Golgi and post-Golgi compartments and are involved in organelle pH regulation. J. Biol. Chem. 2005; 280:1561–1572. [PubMed: 15522866]
34. Numata M, Orlowski J. Molecular cloning and characterization of a novel (Na+,K+)/H+ exchanger localized to the trans-Golgi network. J. Biol. Chem. 2001; 276:17387–17394. [PubMed: 11279194]
35. Ali R, Brett CL, Mukherjee S, Rao R. Inhibition of sodium/proton exchange by a Rab-GTPase-activating protein regulates endosomal traffic in yeast. J. Biol. Chem. 2004; 279:4498–4506. [PubMed: 14610088]
36. Brett CL, Tukaye DN, Mukherjee S, Rao R. The yeast endosomal Na+K+/H+ exchanger Nhx1 regulates cellular pH to control vesicle trafficking. Mol. Biol. Cell. 2005; 16:1396–1405. [PubMed: 15635088]
37. Gilfillan GD, et al. SLC9A6 mutations cause X-linked mental retardation, microcephaly, epilepsy, and ataxia, a phenotype mimicking Angelman syndrome. Am. J. Hum. Genet. 2008; 82:1003–1010. [PubMed: 18342287]
38. Morrow EM, et al. Identifying autism loci and genes by tracing recent shared ancestry. Science. 2008; 321:218–223. [PubMed: 18621663]
39. Franke B, Neale BM, Faraone SV. Genome-wide association studies in ADHD. Hum. Genet. 2009; 126:13–50. [PubMed: 19384554]
40. Takamori S, et al. Molecular anatomy of a trafficking organelle. Cell. 2006; 127:831–846. [PubMed: 17110340]
41. Gronborg M, et al. Quantitative comparison of glutamatergic and GABAergic synaptic vesicles unveils selectivity for few proteins including MAL2, a novel synaptic vesicle protein. J. Neurosci. 2010; 30:2–12. [PubMed: 20053882]
42. Beg AA, Ernstrom GG, Nix P, Davis MW, Jorgensen EM. Protons act as a transmitter for muscle contraction in C. elegans. Cell. 2008; 132:149–160. [PubMed: 18191228]

43. Accardi A, Miller C. Secondary active transport mediated by a prokaryotic homologue of ClC Cl- channels. Nature. 2004; 427:803–807. [PubMed: 14985752]

44. Graves AR, Curran PK, Smith CL, Mindell JA. The Cl-/H+ antiporter ClC-7 is the primary chloride permeation pathway in lysosomes. Nature. 2008; 453:788–792. [PubMed: 18449189]

45. Picollo A, Pusch M. Chloride/proton antiporter activity of mammalian CLC proteins ClC-4 and ClC-5. Nature. 2005; 436:420–423. [PubMed: 16034421]

46. Scheel O, Zdebik AA, Lourdel S, Jentsch TJ. Voltage-dependent electrogenic chloride/proton exchange by endosomal CLC proteins. Nature. 2005; 436:424–427. [PubMed: 16034422]

47. Hell, JW.; Jahn, R., editors. Preparation of synaptic vesicles from mammalian brain. Academic Press; San Diego: 1994.

48. Borst JG, Helmchen F, Sakmann B. Pre- and postsynaptic whole-cell recordings in the medial nucleus of the trapezoid body of the rat. J. Physiol. 1995; 489(Pt 3):825–840. [PubMed: 8788946]

49. Huang H, Trussell LO. Control of presynaptic function by a persistent Na(+) current. Neuron. 2008; 60:975–979. [PubMed: 19109905]

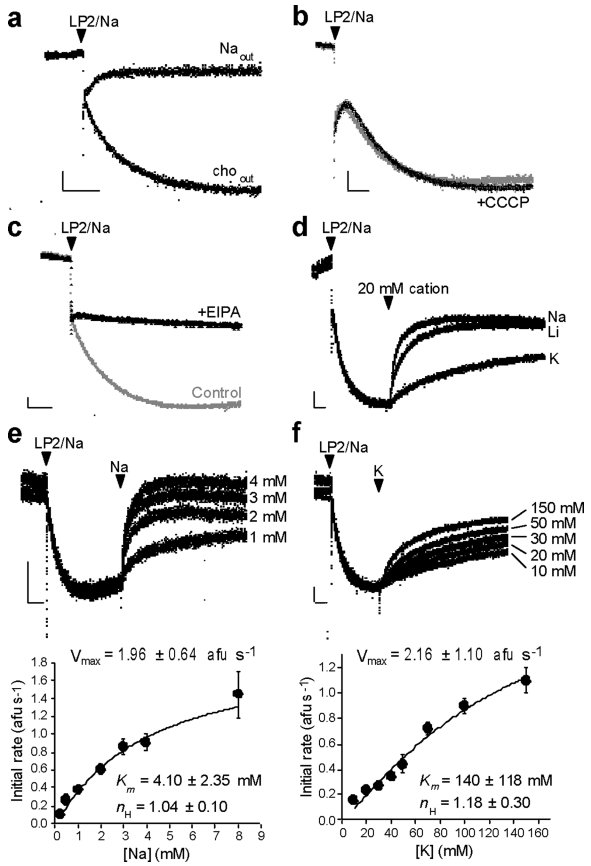

Figure 1. Synaptic vesicles express a Na^+/H^+ exchange activity

Measurement of ΔpH across synaptic vesicles using acridine orange fluorescence. Quenching of fluorescence reflects generation of an inside-acidic ΔpH. Synaptic vesicles preloaded with Na^+ (LP2/Na) and pretreated with bafilomycin to inhibit the V-ATPase were added at the arrowhead to either 150 mM Na gluconate (Na_{out}) or 150 mM choline gluconate (cho_{out}) (**a**), or into 150 mM choline gluconate buffer with or without CCCP (**b**). CCCP does not affect the rate or extent of acidification, indicating that the outwardly directed Na^+ gradient does not drive H^+ flux through changes in membrane potential. (**c**) The acidification of synaptic vesicles by an outwardly directed Na^+ gradient is inhibited by the amiloride analogue 5-(N-ethyl-N-isopropyl)amiloride (EIPA, 15 μM). (**d**) The monovalent cations Na^+, Li^+ and K^+ (20 mM) were added to synaptic vesicles acidified by an outwardly directed Na^+ gradient, as in (**a**). (**e,f**) After acidification as above by an outwardly directed Na^+ gradient, synaptic vesicles alkalinize in a dose-dependent manner to Na^+ (**e**) and K^+ (**f**). The mean initial rates of alkalinization also vary as a function of cation concentration (bottom, n=3), with V_{max}, K_m and Hill coefficient (n_H) obtained by fitting to the Hill equation. All horizontal scale bars indicate 30 seconds; all vertical scale bars indicate 10 arbitrary fluorescence units.

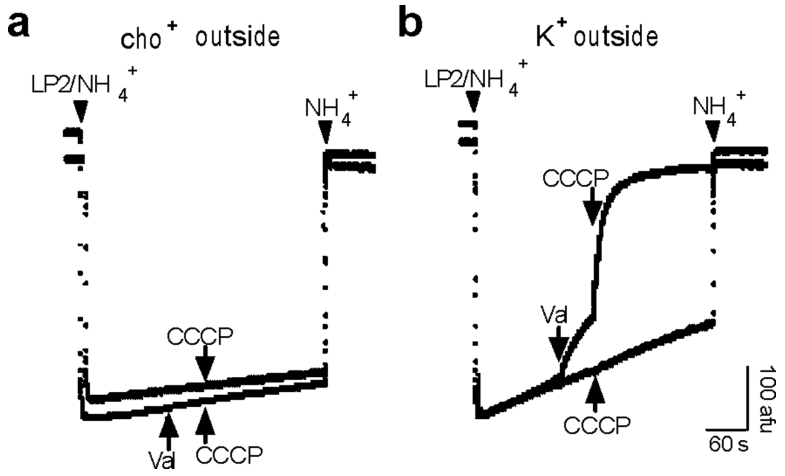

Figure 2. Synaptic vesicles lack a detectable K^+ channel conductance

Measurement of ΔpH across synaptic vesicles using acridine orange fluorescence. Synaptic vesicles were acidified by preloading with 200 mM NH_4^+ (LP2/NH_4^+) and dilution into NH_4^+-free buffer containing (**a**) no K^+ (cho^+ outside) or (**b**) 150 mM K^+ (K^+ outside). In each panel, arrows in the same direction indicate addition to one trace, and arrows in the opposite direction indicate addition to the other trace. CCCP (5 μM) has no effect in the absence of K^+, with or without the addition of 50 nM valinomycin (val). CCCP alone also has no effect in the presence of K^+, indicating the absence of a significant K^+ conductance. However, the prior addition of valinomycin enables CCCP to alkalinize the vesicles rapidly, indicating that CCCP would have produced alkalinization in the presence of an endogenous K^+ conductance. Addition of 100 mM NH_4^+ to the external medium immediately reverses the acidification.

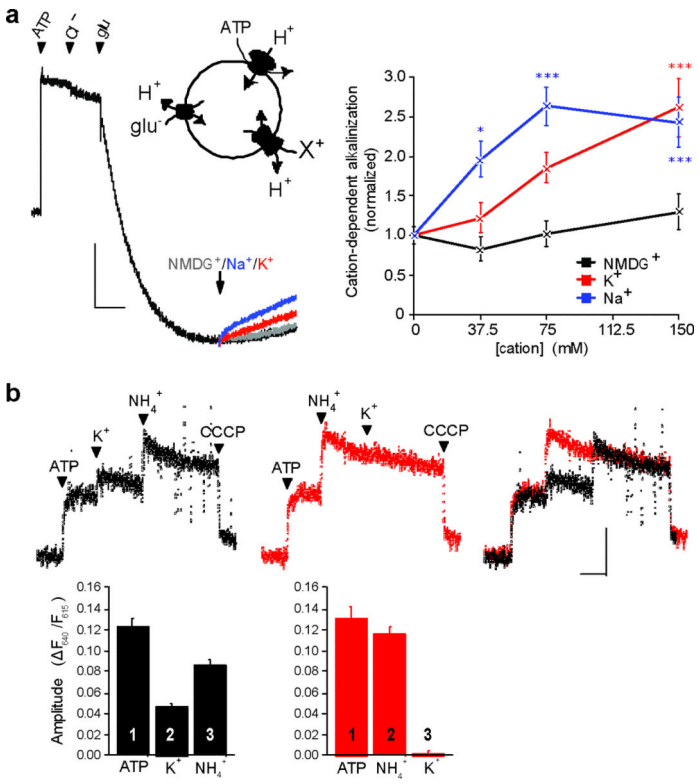

Figure 3. Cation/H^+ exchange activity is present on glutamatergic SVs and increases Δψ

(**a**) The quenching of acridine orange fluorescence shows progressive acidification of 100 μg LP2 protein by 1 mM MgATP, 2 mM choline Cl, and 10 mM choline glutamate (left panel). Gluconate salts of $NMDG^+$ (gray), Na^+ (blue), or K^+ (red) (75 mM final) were added at the arrows, and compared to vesicles that received no additional cation (black). Vertical scale bar indicates 30 arbitrary fluorescence units, horizontal bar, 60 sec. Mean fluorescence change 150 s after the arrow shows that Na^+ and K^+ but not $NMDG^+$ reverse acidification in a dose-dependent manner (right). *, $p<0.05$; ***, $p<0.001$ by two-way ANOVA with post-hoc Bonferroni test. n=6–12 samples (**b**) Synaptic vesicle membrane potential was measured using the ratiometric fluorescence of oxonol VI, with an increase in the ratio reflecting greater inside-positive potential. Arrowheads indicate sequential addition of 1 mM MgATP, 50 mM K gluconate, 10 mM $(NH_4)_2$ tartrate and 5 μM CCCP (left), with the order of K^+ and NH_4^+ addition reversed in the middle panel, and the two traces superimposed on the right. Bar graphs show the mean change in fluorescence ratio, with the order of addition indicated by numbers on or above the bars (n=9 and 4 for left and middle panels, respectively). $p<0.05$ for the effect of NH_4^+ after versus before K^+, and $p<0.0001$ for the effect of K^+ amplitude before and after NH^+_4, by two-tailed unpaired t-test. Vertical scale bar indicates a ratio of 0.10 and horizontal 60 sec. Data are presented as mean ± SEM.

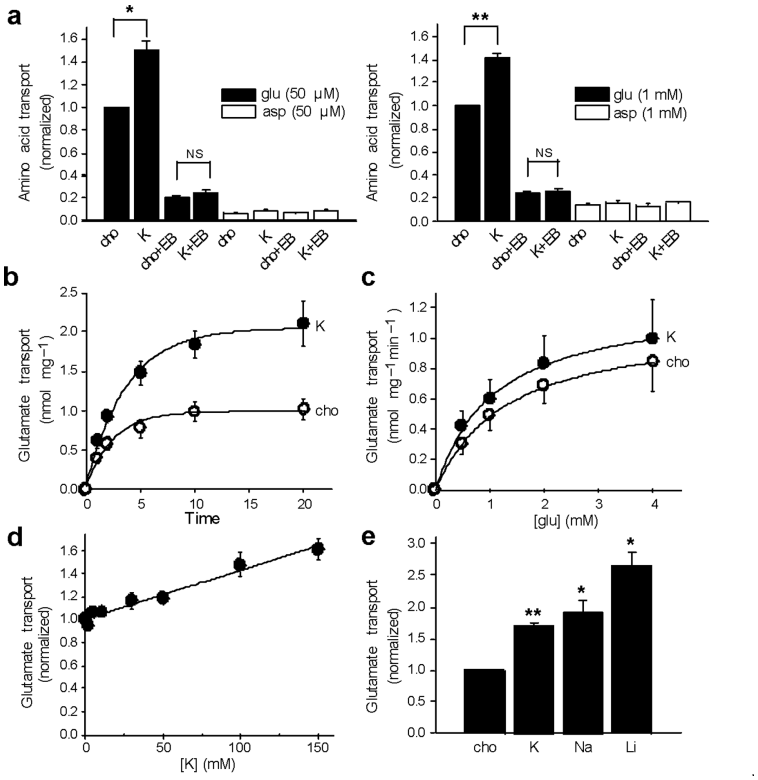

Figure 4. Monovalent cations increase glutamate transport into synaptic vesicles

(**a**) The uptake of ^{3}H-glutamate (filled bars) or -aspartate (open bars) by rat brain synaptic vesicles was measured at 10 minutes in assay buffer containing either 2 mM choline Cl and 148 mM choline gluconate (cho) or 2 mM KCl and 148 mM K gluconate (K), in either 50 μM or 1 mM amino acid, with or without VGLUT inhibitor Evans Blue (EB) (at 10 and 100 μM for left and right panels, respectively). Uptake was normalized to that observed with choline in the absence of Evans Blue. * $p<0.05$, ** $p<0.01$, NS indicates $p=0.11$ for left panel and 0.40 for right. n=3 (**b, c**) Time course (**b**) and kinetics (**c**) of glutamate uptake in either 150 mM choline (open circles) or 150 mM K^{+} (filled circles). The time course was performed using 1 mM glutamate, and the kinetic analysis at 1 minute, yielding mean K_m 1.02 ± 0.08 mM for K and 1.27 ± 0.04 mM for cho ($p<0.05$), and mean V_{max} 1.26 ± 0.33 nmol/mg and 1.12 ± 0.24 nmol/mg for K and cho, respectively ($p=0.31$). n=3 (**d**) Dose response of glutamate uptake to potassium, with total choline and K gluconate adjusted to 150 mM, and uptake normalized to that in no potassium. (**e**) Uptake of 1 mM ^{3}H-glutamate for 10 minutes in the presence of 150 mM K, Na or Li gluconate, normalized to that in 150 mM choline. *, $p<0.05$ and **, $p<0.01$ relative to cho (n=3). Statistical analysis was by two-tailed, paired t-test, and values indicate mean ± SEM.

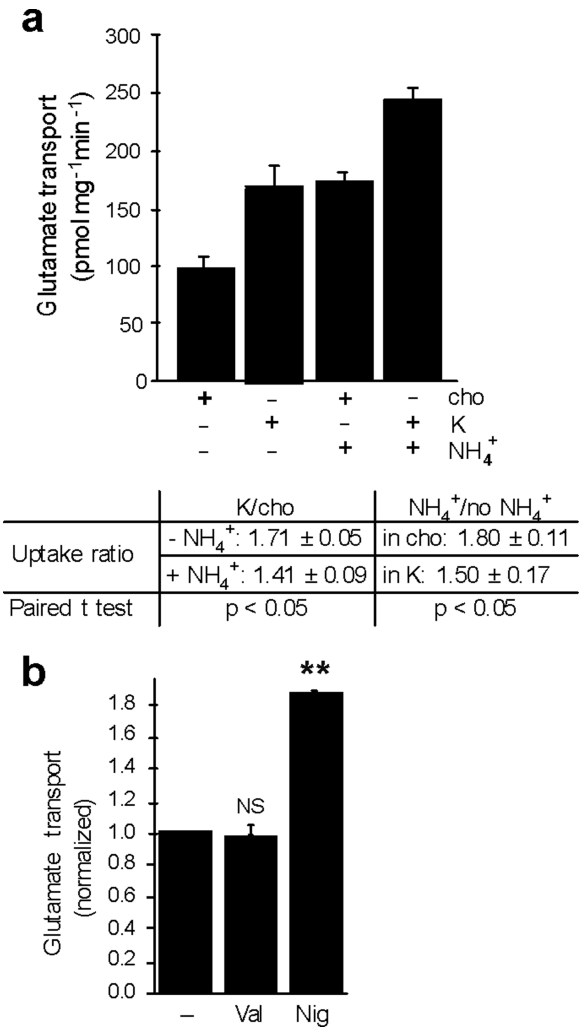

	K/cho	NH_4^+/no NH_4^+
Uptake ratio	- NH_4^+: 1.71 ± 0.05	in cho: 1.80 ± 0.11
	+ NH_4^+: 1.41 ± 0.09	in K: 1.50 ± 0.17
Paired t test	$p < 0.05$	$p < 0.05$

Figure 5. Cation/H^+ exchange stimulates glutamate uptake by increasing Δψ

(**a**) Synaptic vesicle uptake of 1 mM ^{3}H-glutamate was measured in either 150 mM choline or 150 mM K^+, in the presence or absence of 10 mM $(NH_4)_2$tartrate (top). The fold-stimulation of transport by K^+ in the presence or absence of NH_4^+ and by NH_4^+ in the presence or absence of K^+ indicate that NH_4^+ partially occluded the effect of K^+ and vice versa ($p<0.05$ by two-tailed paired t tests, n=4). (**b**) The uptake of ^{3}H-glutamate (1 mM) by synaptic vesicles was measured in 15 mM K gluconate/135 mM choline gluconate with or without either 50 nM nigericin or 50 nM valinomycin. **, $p<0.01$ and NS, $p=0.76$ by two-tailed paired t-tests (n=3). Values indicate mean ± SEM.

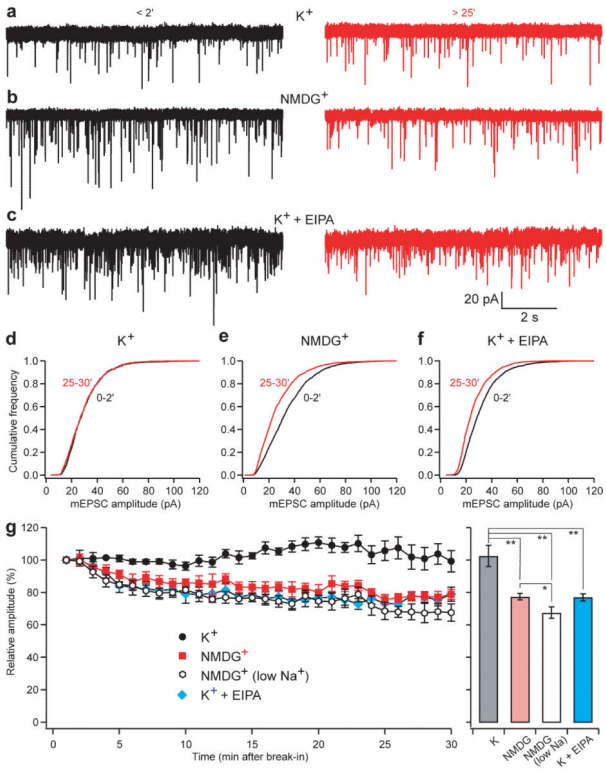

Figure 6. Presynaptic K^+ regulates mEPSC amplitude at the calyx of Held

Paired recordings were performed from both pre- and postsynaptic elements at the calyx of Held. Miniature excitatory postsynaptic currents (mEPSCs) were recorded postsynaptically immediately (within 2 min) and 25–30 min after break-in to the presynaptic terminal with a pipette containing either 130 mM K^+ solution (**a**,**d**), 130 mM $NMDG^+$ (zero K^+) solution (**b**,**e**) or high K^+ solution with 50–100 μM EIPA (**c**,**f**). All presynaptic solutions contained 10 mM Na^+ to mimic physiological conditions. (**a–c**) Recordings made <2 min (left) and 25–30 min (right) after break-in to the presynaptic terminal. Vertical and horizontal space bars indicate 20 pA and 2 s, respectively. (**d–f**) Cumulative probability histograms of mEPSC amplitude early (black) and late (red) during dialysis of the nerve terminal show relatively little difference when the pipettes were filled with high K^+ solution ($p>0.05$, n=4) (**d**), but a shift toward smaller amplitudes with a presynaptic solution low in K^+ ($p<0.001$, n=5) (**e**) or with solution containing high K^+ and EIPA ($p<0.05$, n=4) (**f**). (**g**) Time course of the average data from paired recordings with presynaptic pipettes containing high K^+ (black; n=4), low K^+ (red; n=5) or high K^+ solution with 50–100 μM EIPA (blue; n=4). Each point represents the mean and SEM of recording over the previous 1-min. All presynaptic solutions contained 10 mM Na^+ except for the low Na^+ solution (open; n=5) which contained only 0.6 mM Na^+. *, $p<0.05$; **, $p<0.01$

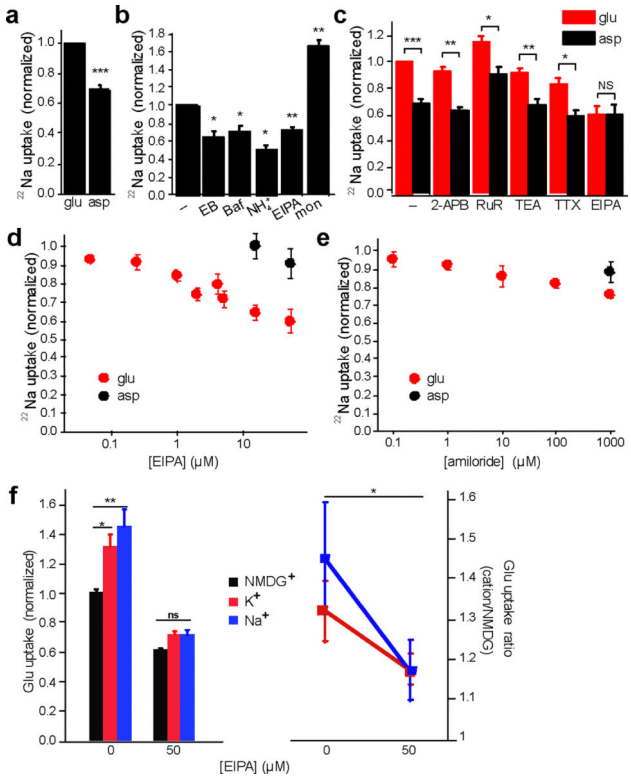

Figure 7. ΔpH-driven $^{22}Na^{+}$ uptake into glutamatergic synaptic vesicles is EIPA-sensitive

Synaptic vesicle uptake of $^{22}Na^{+}$ was measured for 10 minutes in ATP and either 10 mM choline glutamate or 10 mM choline aspartate (**a**), and the results normalized to uptake in glutamate (n=25). (**b**) $^{22}Na^{+}$ uptake was measured in the presence of ATP, glutamate and either EIPA (15 μM), Bafilomycin A1 (Baf) (0.5 μM), Evans Blue (EB) (100 μM), $(NH_4)_2$ tartrate (NH^{+}_4) (10 mM), or the Na^{+} ionophore monensin (mon) (5 μM) as positive control (n=3–5). (**c**) Uptake in 10 mM choline glutamate or aspartate, with and without 2-aminoethoxydiphenylborate (2-APB) (50 μM), ruthenium red (RuR) (100 μM), tetraethylammonium (TEA) (5 mM), tetrodotoxin (TTX) (0.5 μM) and EIPA (50 μM) (n=3–5). (**d**) EIPA inhibits $^{22}Na^{+}$ uptake more potently in vesicles acidified with glutamate (n=3–6). (**e**) Amiloride also inhibits $^{22}Na^{+}$ uptake, but less potently than EIPA (n=5–6). *, $p < 0.05$; **, $p<0.01$ and ***, $p<0.0001$; NS indicates p=0.99 by two-tailed paired t tests. (**f**) The uptake of ^{3}H-glutamate was measured for 10 minutes in assay buffer containing 4 mM MgATP, 2 mM choline chloride, 10 mM glutamate, 10 mM NMDG gluconate and either 150 mM NMDG gluconate (black), 150 mM Na gluconate (blue) or 150 mM K gluconate (red), with or without EIPA. After subtraction of the background in 100 μM Evans Blue, uptake was normalized to that observed in NMDG gluconate without EIPA (left panel). The uptake in Na^{+} or K^{+} was then normalized to that in $NMDG^{+}$ (right panel). *, $p<0.05$; **, $p<0.01$ by two-way ANOVA (n=15–18). Data indicate mean ± SEM.